ORIGINAL RESEARCH ARTICLE

Barycenter reflected equatorial Pacific sea level structure evolution and its indication of ENSO events ☆

Wen Luo [a,c], Lin Yi [a], Zhaoyuan Yu [a,b,*], Hui Sun [a], Linwang Yuan [a,b]

[a] Key Laboratory of Virtual Geographic Environment, Ministry of Education, Nanjing Normal University, Nanjing, PR China
[b] Jiangsu Center for Collaborative Innovation in Geographical Information Resource Development and Application, Nanjing, PR China
[c] Geography Department, University of Wisconsin-Madison, Madison, United States

Summary   Focused on the zonal and meridional response of sea level change to El Niño-Southern Oscillation (ENSO) events, this paper retrieves the overall average, positive anomaly and negative anomaly sea surface height (SSH) series of equatorial Pacific area (EPA) from satellite altimetry data from 1993 to 2013. The barycenter method is then applied to each of the three series to get the zonal and meridional barycenter coordinates. The barycenter coordinates are then compared with the Multivariate ENSO index (MEI) to reveal the zonal and meridional response of sea level change to ENSO. The meridional and zonal spatio-temporal evolutionary processes of sea level change in EPA during different ENSO events are reconstructed by the Principle Tensor Analysis of Rank 3 Method (PTA3). Comparative analysis shows that the meridional change of positive anomalies barycenter, rather than the mean series of sea level height anomaly in EPA, can well characterize the intensity and evolutionary process of ENSO events. Meanwhile, the zonal migration of barycenter may reflect the lag adjustment of the sea level to the ENSO signal. The analysis on the meridional and zonal evolution of the sea level change in different ENSO periods shows that the response of sea level change to the ENSO events can be mainly characterized by the position differences between positive and negative sea level anomaly barycenter, SSH gradient in the meridional direction and the inconsistency in the overall spatial structure and temporal evolution characteristics in the zonal direction.
© 2015 Institute of Oceanology of the Polish Academy of Sciences. Production and hosting by Elsevier Sp. z o.o. All rights reserved.

ELSEVIER | **Production and hosting by Elsevier**

1. Introduction

Revealing the overall features and main patterns of spatial-temporal process of ENSO events is important. ENSO events are atmosphere-ocean coupling events that occurred at the equatorial Pacific and with global impact (Yadav et al., 2013). Most of studies focus on the spatial-temporal structure, dynamical evolution processes, model simulation and impact evaluation of ENSO (Chowdary et al., 2014; Paeth et al., 2008; Wang et al., 2006). Recently, typical ENSO and ENSO Modoki are distinguished. These different ENSO-related events will lead to different spatial-temporal characteristics (Ashok et al., 2007). The amplitudes, phases, evolution processes and impacts of these ENSOs are different, which also leads to the different responses (Chang et al., 2013).

The studies of sea level change are conductive to revealing the spatial-temporal structure and process mechanism of ENSO events owing to its sensitive responsiveness (Rong et al., 2007; Yuan et al., 2009; Zhang and Church, 2012). Different from other indexes (e.g. Sea Surface Temperate (SST)), the sea level can effectively avoid the atmospheric fluctuations (Ji et al., 2000) and provide high quality data for logging the responses to significant irregular oscillation of atmosphere-ocean coupling events (e.g. Madden-Julian Oscillation (Oliver and Thompson, 2010)), changes in ocean circulation (e.g. Rossby waves (Bosc and Delcroix, 2008; Singh et al., 2013)), etc. The model simulation experiments also suggest the significance of integrating the sea level data into the global and regional model simulations for more accurate output for ENSO simulation and prediction.

The mean sea level height anomaly (MSLA) series are most commonly used index for revealing the sea level change and its response to ENSO events. Since 1970s, the MSLA series reconstructed from the tide gauge data have become an important indicator of ENSO studies (Losada et al., 2013; Lu et al., 2013; Luo et al., 2011; Wyrtki, 1975). Satellite altimetry data, which have more spatial resolutions, are also used to study the spatio-temporal revolution of ENSO (Andersen and Cheng, 2013; Cazenave and Nerem, 2004; Nerem, 1999; Yu et al., 2011). Some recent works, which reconstruct high resolution spatio-temporal MSLA series by combining both the tide gauge and satellite altimetry data, also reveal the spatio-temporal evolution of ENSO in global and regional scales (Church et al., 2005; Rong et al., 2007).

However, as a time domain only index, the MSLA cannot reveal the zonal and meridional coupling evolution characteristic and high and low values of sea level change correspondent to the ENSO. The MSLA is mainly obtained by averaging sequence of regional SSHA through direct spatial average or extracting the dominant spatio-temporal modes based on Empirical Orthogonal Function (EOF)-like methods (Takahashi and Morimoto, 2013). The direct spatial average method, performed in one dimension, ignores the spatial heterogeneity of eustacy. The EOF-like methods, which project the data into two-dimensional matrix, can only reveal the significant average characteristics and are difficult to create the precise structure of eustacy (Kim and Wu, 1999; Puillat et al., 2014).

The impact of ENSO signal on sea level change has the characteristics of asymmetry, irregularity and quasi-periodicity (Liu et al., 2006). ENSO signal will inevitably lead to a corresponding asymmetry in the deviation degree of positive or negative sea level fluctuation anomaly from the mean sea level height in the spatio-temporal domain. Taking into account positive and negative anomalies of sea level change, analyzing the structural features and process information of its spatio-temporal evolution and discussing the correspondence and similarity between this index and ENSO index, will have the potential to provide more detailed information about the response characteristics and structural process between the sea level changes and ENSO.

In this paper, we divide the SSH data in EPA into three different catalogs: the overall anomaly, positive anomaly and negative anomaly according to the overall average baseline to separately reveal their different responses to ENSO. Then the barycenter method is applied to reveal the zonal and meridional evolution characteristics of sea level series of different catalog. Then, the meridional and zonal evolution characteristics of the sea level change during different ENSO events are discussed. The paper is organized as follows: Section 2 presents the introduction of used research data and methods. Section 3 provides the analysis results, including the spatio-temporal evolution characteristics of SSHA in EPA, spatio-temporal evolution of different sea level changes and their correlations with ENSO Events, and the process of sea level change during typical ENSO events. Discussion and conclusions are presented in Sections 4 and 5, respectively.

2. Research data and methods

2.1. Research data

The Ref version $1/4° \times 1/4°$ gridded SSHA data, produced by SSAlto/Duacs, AVISO, are used in this paper. The spatial area, EPA, located between 10°S—10°N and 150°E—105°W, and the time period from October 1992 to April 2013, are selected as the research data. Monthly SSHA data are obtained by averaging the data in the same month. MEI (Wolter and Timlin, 1998), provided by the U.S National Oceanic and Atmospheric Administration Earth System Research Laboratory (NOAA ESRL), is used as the ENSO index. Compared with the SOI index, MEI can better reflect the process of starting and dying of ENSO, and can also well reflect the strength of ENSO events (Ortiz-Tánchez et al., 2002). According to the MEI rank values, typical ENSO events occurred during the overall research are identified. The time coefficients of the first and second principal components extracted by PTA3 method (Leibovici, 2010; Yu et al., 2011) are used as references for the zonal and meridional evolution of ENSO.

2.2. Barycenter analytic method

Barycenter analytic method is a commonly used geographic spatial analysis method, by which, the spatial distribution of the geoscience indexes is used as the weight to calculate the barycenter coordinates. The coordinates of the barycenter can reflect the average location information of space effect of index. The migration process of barycenter over time reflects the process of restructuring or moving of index in spatial distribution. If the attribute analyzed changes smoothly (i.e. the amplitude changes over the space are not very shape), the barycenter is relatively stable.

The barycentric coordinates can be obtained simply by the weighted average of observed index and space coordinates. For two-dimensional spatial points, the barycentric coordinates can be computed as follows:

$$X_G = \frac{\sum_i W_i X_i}{\sum_i W_i}, \qquad Y_G = \frac{\sum_i W_i Y_i}{\sum_i W_i}, \tag{1}$$

where X_G and Y_G are barycentric coordinates of the observing index. W_i is the weight of the point at location i, X_i, and Y_i are the original coordinates of the data at location i. In this paper, the SSHA at each grid of the satellite altimeter data can be used as the weight W_i, and therefore, the computed X_G and Y_G are the barycentric coordinates of the sea level anomaly. The migration of the barycenter in the given area can reveal the dynamic change characteristics of sea level.

2.3. The cross wavelet spectrum method

Cross wavelet spectrum and wavelet coherence analysis are multiscale mutual information processing methods based on the wavelet transformation. The two methods can reveal the multiscale power covariance and coherent relations as well as phase relations between two time series (Grinsted et al., 2004). The covariance and coherent relations as well as the phase relations can then provide the information about the consistency and correlations in time-frequency space at different scales and different times.

Assuming $W_n^X(s)$ and $W_n^Y(s)$ are the continuous wavelet transformation of two time series X_n and Y_n, the cross wavelet spectrum is defined as:

$$W_n^{XY} = W_n^X(s) W_n^{Y*}(s), \tag{2}$$

where $W_n^{Y*}(s)$ is the complex conjunction of $W_n^Y(s)$. Therefore, the power of this cross spectrum $|W_n^{XY}(s)|$ reveals the power resonance between X_n and Y_n in the time-frequency space. The complex angle of W_n^{XY} represents the local phase information in the time-frequency space.

The wavelet coherence is defined as:

$$R_n^2(s) = \frac{|S(s^{-1} W_n^{XY}(s))|^2}{S(s^{-1}|W_n^X(s)|^2) \cdot S(s^{-1}|W_n^Y(s)|^2)}, \tag{3}$$

where S is the smoothing operator. The definition of the wavelet coherence is similar to the classical correlation coefficients, which reveals the local correlations in the time-frequency space.

2.4. The data processing procedure

The whole data processing procedure is based on the barycenter coordinates computation for SSH data. The overall SSHA time series average of each grid in EPA is first calculated as long-term baseline grid of the sea level eustacy. Then the data are divided into the positive anomaly part (greater or equal to long-time average baseline) and the negative anomaly part (lower than long-time average baseline) for each grid point at each time. Thus we have the overall SSHA grid series, positive anomaly grid series and the negative anomaly grid series of MSLA in EPA. The zonal and meridional barycenter coordinates series, with each of the three grid series at each time computed according to Eq. (1), are computed to reveal

the spatial distribution and temporal evolution of the SSHA. Thus, we have totally three zonal and three meridional barycenter coordinate time series that reveals the zonal and meridional migration of the overall SSHA, positive anomaly and the negative anomaly. To better reveal the relations between SSHA, barycenter coordinate series and ENSO, the spatial average mean series of the overall SSHA grid series, positive anomaly grid series and negative anomaly grid series are also computed. The three mean series as well as six barycenter coordinate time series are compared with MEI index. Then the temporal and spatial migration of the barycenter coordinates and their relations with ENSO evolution are discussed.

3. Results

3.1. The spatio-temporal evolution characteristics of SSHA in EPA

The comparisons between the spatial mean series, the barycenter coordinates of the three grid series and the MEI index are depicted in Fig. 1. The result suggests that the mean series of SSHA in the whole EPA has a certain comparability with the MEI index in the overall structure yet with particular volatility. The overall mean series is in phase with MEI series during El Niño events and anti-phase in the rest of the time. In respect of structure and trend, the overall mean series has a clear trend and decadal scale fluctuations, while the MEI index only has slight fluctuation. The positive anomaly, which mainly displayed as low-frequency interannual-decadal-scale fluctuations, has a good correspondence with the MEI index in the peak. Negative anomaly of the sea level, which has significantly lower volatility of positive anomaly, was stable. During the study, the negative anomaly series, which lags MEI index changes on the whole, had a significant fluctuating only from 1997 to 1998. From 2002 to 2006, the amplitude of the negative anomaly is close to 0, and this period is the least active period of ENSO. The asymmetry of positive and negative sea level anomalies shows that their responses to ENSO events are significantly different.

As Fig. 1b, c shown, the correlation between the zonal barycenter change of positive and negative sea level anomaly and MEI index is poor. The zonal change of the positive sea level anomaly suggests a clear yearly fluctuation. A large trough occurred in 1998 alone, when the sea level barycenter reaches 8°S in the farthest. In late 2001, its zonal scope of movement significantly narrowed, basically only in 1°N−1°S. The low-frequency fluctuation of negative sea level anomaly was significantly higher than the positive sea level anomaly change. After the strong El Niño during the period from 1997 to 1998, the barycenter showed trend toward the south side, which may reflect the lasting impact of the strong ENSO events. From 2003 to 2006, abnormal fluctuation in frequency variation appeared in the negative sea level barycenter.

There is a high consistency between the meridional movement of positive sea level anomaly and MEI index in both structure and volatility particulars. This appearance indicates that the meridional movement of the positive sea level anomaly barycenter in EPA can reveal the change and strength of ENSO. Seen from the geographical position of positive sea level anomaly barycenter, the positive sea level
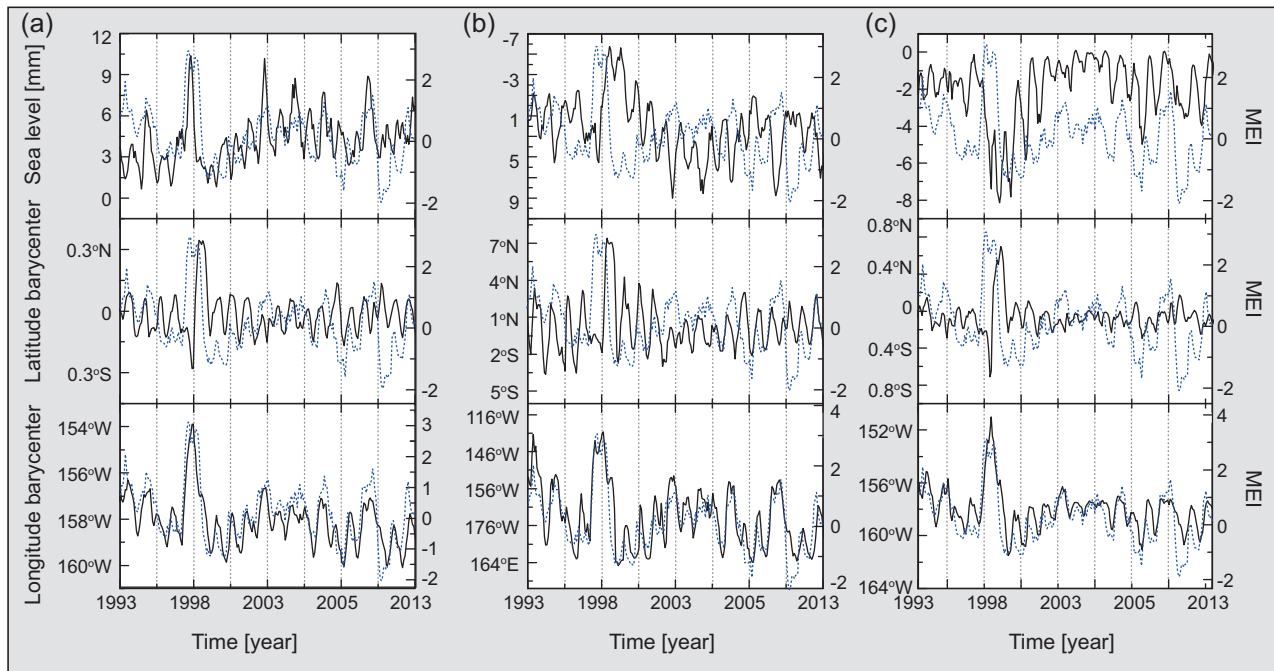
Figure 1 The comparison of the different averaged SSHA series, the coordinate series of the barycenter and the MEI index. (The solid lines are the averaged SSHA and the barycenter coordinate series and the dash lines are the MEI index.) The result suggests that the mean series of SSHA in the whole EPA has lower comparability with the MEI index than positive anomaly series. The positive anomaly series corresponded with MEI well even in peaks, and thus can largely reflect the spatio-temporal change of ENSO. Negative anomaly of the sea level was relatively stable. (a) The whole data. (b) The positive anomaly data. (c) The negative anomaly data.

anomaly barycenter was in the west of 150°W during the strong ENSO period from 1997 to 1998. The meridional movement of negative sea level anomaly barycenter also had a good comparability with the MEI index. However, the meridional movement of negative sea level anomaly did not show clear trends or inter-annual fluctuations. In the none-ENSO period from 2003 to 2006, weak frequency changes appeared in the negative sea level anomaly barycenter series.

3.2. Spatio-temporal evolution of sea level change and its correlation with ENSO events

The zonal and meridional coordinates of positive sea level anomaly barycenter have good correspondence with the time coefficients of the first and second principal components extracted by PTA3 method (Fig. 2). The results show that the meridional and zonal migration based on the positive sea level anomaly barycenter can characterize the evolution of sea level change from both directions. The meridional change of the barycenter has a high correspondence with the MEI index, while the zonal change of the barycenter has a significantly weakened correspondence with MEI. A five-month lag, which can be observed in many different regions (Holbrook et al., 2011; Rong et al., 2007), can also be found between meridional change of the barycenter and MEI index. Meanwhile, the phase relationship between the zonal coordinate series of the barycenter and the MEI index is inconsistent in structures. It manifests as the anti-phase in the occurring period of ENSO events and as synchronous changes in the none-ENSO period. The meridional movement of the water body in the ENSO period may cause a change in the direction of the

zonal ocean circulation, leading to the emergence of anti-phase. The lag between the quick adjustment of meridional barometric gradient and the adjustment of baroclinic Rossby wave produced in the Middle East equatorial region (Masuda et al., 2009), and the phase difference between the zonal Ekman circulation and stratospheric transmission (Masuda et al., 2009) may also be the reasons for the lag.

The principal tensor reconstruction, superimposed with zonal and meridional coordinates of corresponding positive SSHA barycenter, is conducted to get the temporal-meridional and temporal-zonal evolution of sea level changes in EPA (Fig. 3a, b). The positive SSHA barycentric migration, which shows a significant volatility, has a good correspondence with the time-meridional and time-zonal structure. The zonal and meridional trajectories fluctuate at 170°W and 0° nearby respectively. The maximum of zonal and meridional trajectory deviation occurred between 1997 and 1998, corresponding with the strong El Niño event from 1997 to 1998. The meridional coordinate maximum was 133.42°W (February 1998), while the zonal fluctuations reached the maximum in the north in May 1998 (7.29°N). The extreme value of zonal trajectory has corresponded well with the ENSO events. The sea level height difference was also most obvious at this time. The period from 1998 to 2003 also contained a weak El Niño event, La Niña event and none-ENSO period between them, so the meridional and zonal fluctuations of the sea surface barycenter were intense. Since April 2002, significantly low sea level area appeared in equatorial Pacific, the SSHA in the west of 150°E was below 4 mm. The reversal of "high south and low north" zonal fluctuation appeared from April 2003, and then it started a long none-ENSO period, confirming the possible negative
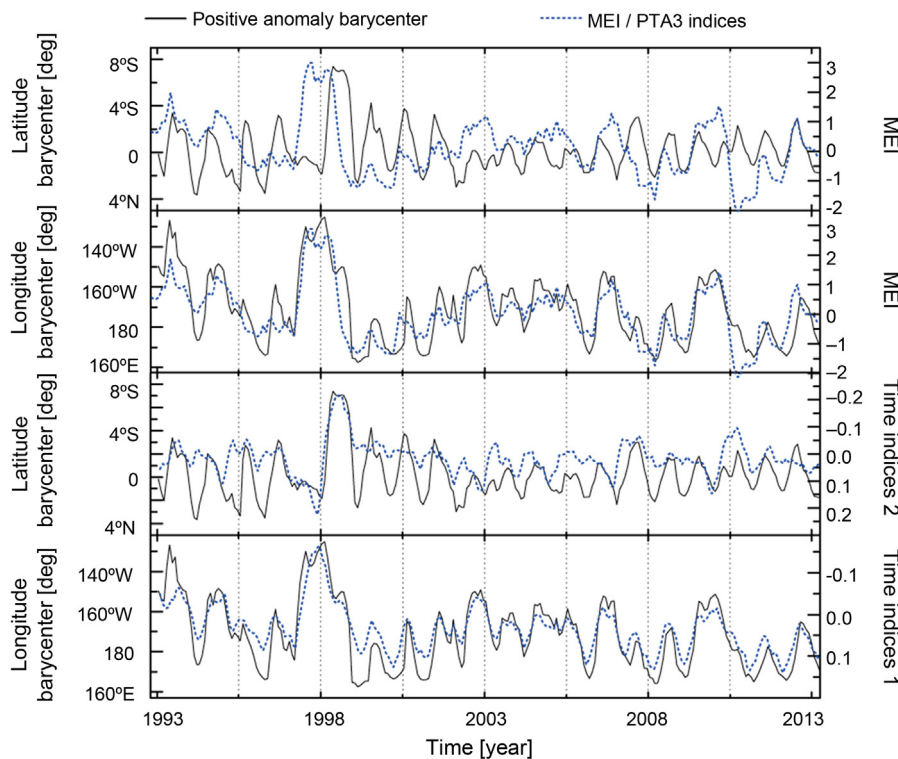
Figure 2 The comparison of the temporal coefficients of PTA3 decomposition and related indexes. The meridional change of the barycenter has a high correspondence with the MEI index, the correspondence between the zonal change and the MEI index is significantly weakened. A five-month lag exists between meridional change of the barycenter and MEI index.

feedback of zonal transfer of sea level change on ENSO events.

The cross wavelet spectrum and cross coherence spectrum between the zonal and meridional coordinates series of positive sea level anomaly are calculated to further clarify the structural characteristics of the series (Fig. 3c, d). The coherence relations of zonal and meridional barycenter movement show that the zonal and meridional barycenter coordinates series have a continuous coherence relation in the annual cycle, in which meridional change starts about five months in advance of the zonal change in phase. The continuous coherence relation in the annual cycle is broken from 1997 to 1999, which may suggest a common response of the zonal and meridional movement of sea level change to strong ENSO events. The zonal and meridional barycenter coordinates had clear power resonance relations in the scales of 2.6 years and more than 4 years before 2002. The meridional change was in advance of zonal change. After 2002, the power resonance relationship between them disappeared. The coupled multisclae interaction between zonal and meridional barycenter coordinates also agrees well with the statement that the sub-strong El Niño event may be the combined result of a variety of modes (Masuda et al., 2009).

3.3. The process of sea level change during typical ENSO events

During the period from March 1997 to May 2003, several ENSO events took place, including the 97—98 strong El Niño event

from March 1997 to July 1998, the weak El Niño event from May 2002 to May 2003 and the weak La Niña events from September 1998 to March 2000 Using the spatial pattern of the first (meridional) and second (zonal) principal tensor obtained by PTA3 with the tensor product, the meridional and zonal component data of sea level change in this period was reconstructed. By overlaying the zonal and meridional barycenter migration series (Fig. 4), we can explore the process of the generation, development and demise of different types of ENSO events to reveal possible relations between sea level changes and ENSO events.

The strong El Niño during 1997—1998 started from the West Tropical Pacific, and reached the maximal intensity in October 1997, at which time the scope of sea anomalies area extended to about 175°W and the amplitude of the SSH difference was more than 50 cm. The PTA3 reconstruction of meridional spatio-temporal change showed that this El Niño event expanded from the eastern Pacific Ocean to the middle and western Pacific, which can be also reflected from the barycenter position change in both positive and negative anomalies. The morphological structure and amplitude of the zonal sea level changed slightly during the period of the emergence and development of the event. The zonal variation of the sea level increased gradually, and significant low sea level anomaly appeared in the south since February 1998. The low sea level anomalies extended to the maximum from April 1998. In the meantime, the first principal tensor of the sea level is close to the average sea level, and the sea level anomalies in the east and west were broadly consistent. After May 1998, the meridional component of the western
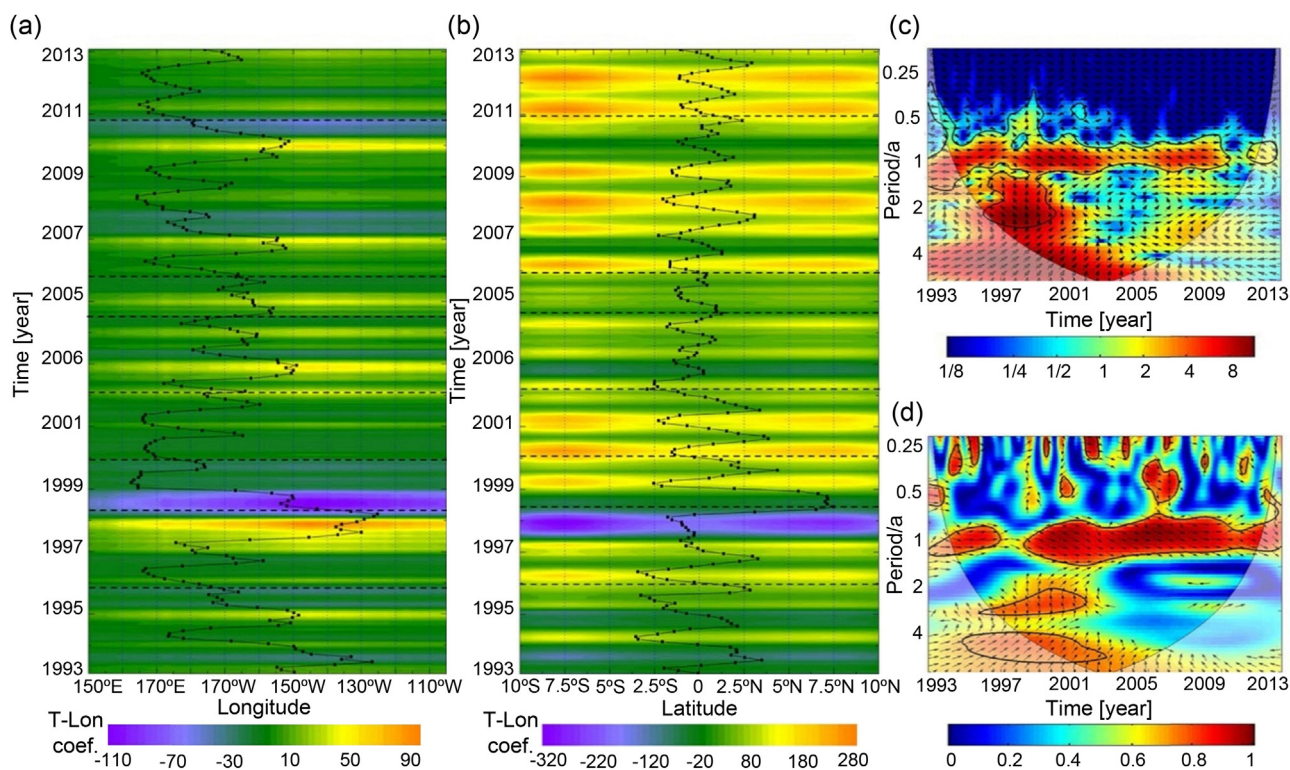
Figure 3   The comparison of the coupled processes of longitudinal and latitudinal sea level change. The respective color in the left and middle graph represent the longitudinal-time and latitude-time evolution, reconstructed from the PTA3 coefficients by the tensor product. The black line on the graph shows the longitude and latitude coordinates of barycenter changes through time. In the right graph, the color indicates the value of cross spectrum or the wavelet coherence. The vectors indicate the phase difference, a horizontal arrow pointing from left to right signifies in-phase and an arrow pointing vertically upward means the zonal and coordinates lags meridional coordinates by 90°. The thick black curve is the region of 95% confidence interval. (a) Longitude barycenter of positive anomaly data. (b) Latitude barycenter of positive anomaly data. (c) Result of cross wavelet transform. (d) Result of wavelet coherence. (For interpretation of the references to color in this figure legend, the reader is referred to the web version of the article.)

Pacific Ocean gradually increased, and the sea level gradually returned to normal levels. In the zonal component, the southern low sea level anomaly persisted, foreshadowing the lag impact of 1997−1998 El Niño on the sea level.

The 2002−2003 weak El Niño events mainly started from the Pacific Ocean. As are shown in the original sea level data, small pieces of high sea level anomaly began to appear in the southwestern region since May 2002, and then the entire southern equatorial sea level began to rise. The mid-equatorial Pacific sea level reached the maximum (near 40 cm above mean sea level) in October 2002. Since January 2003, the area with high sea level anomaly gradually subsided, and the El Niño entered the demise period. For the principal tensor reconstructions, the overall structure of meridional component has relatively small changes. The center of the increasing sea level during the El Niño always remains in 170°W nearby and the sphere of influence of the sea level is concentrated between 5°N and 5°S. As to the zonal component, high sea level center was found in about 8°S, 175°E except in February 2003. The sea levels in other regions were lower or close to the average.

In the 1998−2002 La Niña events, the original sea level data show that there were two obvious sea level anomalies in the periods from December 1998 to May 1999 and from November 1999 to March 2003, which are reflected in the meridional and zonal reconstruction data. From August to

October in 1998, the meridional sea level anomaly showed a "low west and high east" El Niño trend with 180°W as the dividing line. While the zonal variation was quite dramatic: significant high sea level anomaly area appeared in north of 5°N while significant 10°W sea level anomaly area appeared in south of 5°N. The height difference between them was weakened monthly, and the zonal SSH difference almost disappeared in December 1998, suggesting the emergence of a molding La Niña event. The meridional sea level elevation difference became clear gradually during the period from December 1998 to June 1999, and reached the highest level in March 1999, when the zonal sea level variation was relatively stable and the SSH was close to the average sea level. From July 1999, high sea level anomaly area appeared again in southern region of zonal component till the formation of the second La Niña event in December 1999. The zonal "high south and low north" sea level gradient appeared ahead of La Niña events, which may have reference significance to the forecast of La Niña events.

4. Discussions

In this paper, the barycenter analysis is applied to the overall mean, the positive and negative SSHA grid series to extract the zonal and meridional evolution of sea level change. The
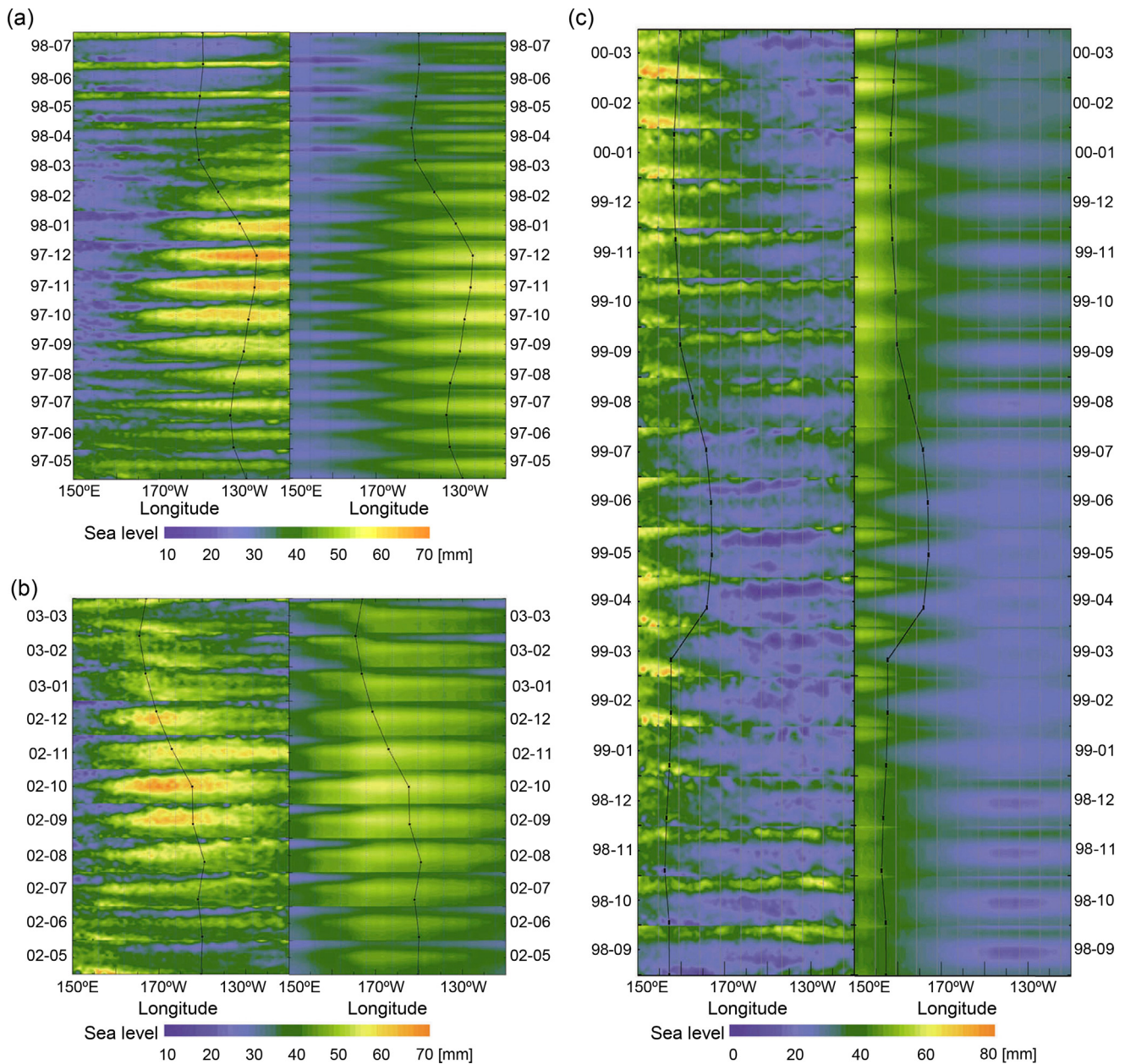
Figure 4 The comparison of the spatio-temporal structure of different types of ENSO events. The color in the graph is the reconstructed sea level height. The thick line on the graph is the coordinate of the barycenter. The graph suggests well that the barycenter coordinates are well corresponding with the high and low of sea level as well as their zonal and meridional evolutions. (a) Reconstructed sea level and the gravity center during El Niño period (97–98), i.e. 1997–1998 - data on the vertical scales. (b) Reconstructed sea level and the gravity center during El Niño period (02–03), i.e. 2002–2003 - data on the vertical scales. (c) Reconstructed sea level and the gravity center during La Niña period (98–00), i.e. 1998–2000 - data on the vertical scales. (For interpretation of the references to color in this figure legend, the reader is referred to the web version of the article.)

result suggests that the barycenter analysis can well reveal the zonal and meridional coupling evolution of SSHA as well as their relations to the ENSO events. The barycenter analysis is simple and stable for long-term operations. The meaning of the barycenter coordinates is direct and clear. Therefore, it can be used as a common operational analysis for sea level and even other similar climate and oceanographic indexes. It also has the potential to be a standard index that indicates the spatio-temporal evolution of SSHA and ENSO in EPA.

Studying the ENSO responses based on the traditional sea level change mean series is relatively homogeneous. In contrast, the positive and negative SSHA barycenter series can not only reveal sea level change response to ENSO events, but also provide the detailed process of meridional and zonal interaction of sea level change. In our result, even in EPA, only a weak correlation is shown between the regional mean sea level anomaly series and the MEI. Seasonal changes in the mean sea level series, the long-term trends and the impact of other noise signals can be the reason for the poor correspondence.

Compared with MSLA, the mean series of the positive and negative anomalies of the sea level change can reflect more structural information in the sea level change. The positive anomalies series have a good correspondence with MEI index and may reflect the direct drive action of the ENSO on the sea; while negative anomalies series may only be affected by the strong ENSO events and reflect a stable response of the sea level change to the ENSO.

Sea level changes sensitively respond to the coupled interaction between atmosphere and ocean (Nerem et al., 2006). Ocean thermal conditions, the wind field, pressure field within the region, and associated changes in atmospheric circulation and ocean currents can affect the distribution of sea-level change (Xu et al., 2012). The mass transfer and thermocline variations of equatorial Pacific are important factors in the ENSO generation and development process. The comparison of the barycenter migration between the positive and negative anomaly shows that in the El Niño period, the zonal transmission based on the wind-driven ocean circulation transport mechanism is not symmetrically spread from the equator to both sides, but with a zonal gradient. For example, in the strong El Niño period from 1997 to 1998, the barycenter of positive sea level anomaly is close to 7°S, while the negative barycenter is only shifted to 3°N nearby. This result has, to some extent supported the recharge-oscillator theory. Burgers et al. (2005) discovered that the zonal migration of the water bodies in this area can support the charge-recharge-oscillator theory. They suggested that the zonal change of sea level is consistent with the whole process of ENSO production, occurrence and development. Further studies need to be done including: (1) what is the impact strength and action process of the zonal change of sea level on the ENSO events; (2) the phase relations between positive and negative anomaly sea level meridional change and the MEI index.

This study shows that the stability of the meridional change in the negative SSHA barycenter is significantly higher than the meridional change series of positive SSHA barycenter. According to the observational data and model simulation data, Karnauskas and Busalacchi (2009) pointed out that EPA SST is inconsistent with sea level pressure (SLP) gradient. From 1880 to 2005, the east-west equatorial Pacific SST gradient showed an increasing trend in the autumn, while the SLP gradient remained relatively stable. Bosc and Delcroix (2008) thought that EPA warm water volume change is the result of joint action of meridional circulation and zonal circulation, and they demonstrated the inconsistencies between the action mechanism of pressure gradient and temperature gradient on the warm water volume. They also discussed the relationship between the result and the recharge/discharge oscillator theory based on the satellite altimetry data and the measured data. Further discussion needs to be done about whether differences exist between the impacts of SST and SLP on the equatorial Pacific positive and negative SSHA, and their specific action process and mechanism on both SSHA migrations.

5. Conclusions

This paper efficiently extracted the ENSO signal from the SSHA data of EPA using the barycenter analysis method. The spatio-temporal process of meridional and zonal SSHA and ENSO variations are reconstructed and compared. The results show that the barycenter analysis method can well reflect the whole spatio-temporal change process, including the occurrence, development and demise stages, of ENSO evolution. The extracted spatio-temporal process and dynamic change characteristics of various types of ENSO evolution can reveal the atmosphere-ocean interaction process and the possible mechanisms of ENSO occurred in EPA. The method provides a simple and efficient way for further analyses of factors and mechanisms of meridional and zonal changes of SSH and ENSO.

Acknowledgments

References

Andersen, O.B., Cheng, Y., 2013. Long term changes of altimeter range and geophysical corrections at altimetry calibration sites. Adv. Space Res. 51 (8), 1468—1477.

Ashok, K., Behera, S.K., Rao, S.A., Weng, H., Yamagata, T., 2007. El Niño Modoki and its possible teleconnection. J. Geophys. Res. 112 (C11), C11007.

Bosc, C., Delcroix, T., 2008. Observed equatorial Rossby waves and ENSO-related warm water volume changes in the equatorial Pacific Ocean. J. Geophys. Res. 113 (C6), C06003.

Burgers, G., Jin, F.-F., van Oldenborgh, G.J., 2005. The simplest ENSO recharge oscillator. Geophys. Res. Lett. 32 (13), L13706.

Cazenave, A., Nerem, R.S., 2004. Present-day sea level change: observations and causes. Rev. Geophys. 42 (3), RG3001.

Chang, Y.-T., Du, L., Zhang, S.-W., Huang, P.-F., 2013. Sea level variations in the tropical Pacific Ocean during two types of recent El Niño events. Glob. Planet. Change 108, 119—127.

Chowdary, J., Parekh, A., Gnanaseelan, C., Sreenivas, P., 2014. Inter-decadal modulation of ENSO teleconnections to the Indian Ocean in a coupled model: special emphasis on decay phase of El Niño. Glob. Planet. Change 112, 33—40.

Church, J.A., White, N.J., Arblaster, J.M., 2005. Significant decadal-scale impact of volcanic eruptions on sea level and ocean heat content. Nature 438 (7064), 74—77.

Grinsted, A., Moore, J.C., Jevrejeva, S., 2004. Application of the cross wavelet transform and wavelet coherence to geophysical time series. Nonlinear Process. Geophys. 11 (5/6), 561—566.

Holbrook, N.J., Goodwin, I.D., McGregor, S., Molina, E., Power, S.B., 2011. ENSO to multi-decadal time scale changes in East Australian Current transports and Fort Denison sea level: oceanic Rossby waves as the connecting mechanism. Deep Sea Res. Part II: Top. Stud. Oceanogr. 58, 547—558.

Ji, M., Reynolds, R.W., Behringer, D.W., 2000. Use of TOPEX/Poseidon sea level data for ocean analyses and ENSO prediction: some early results. J. Clim. 13 (1), 216—231.

Karnauskas, K.B., Busalacchi, A.J., 2009. Mechanisms for the inter-annual variability of SST in the east Pacific warm pool. J. Clim. 22 (6), 1375—1392.

Kim, K.-Y., Wu, Q., 1999. A comparison study of EOF techniques: analysis of nonstationary data with periodic statistics. J. Clim. 12 (1), 185—199.

Leibovici, D.G., 2010. Spatio-temporal multiway decompositions using principal tensor analysis on k-modes: the R-package PTAk. J. Stat. Softw. 34 (10), 1—34.

Liu, Q., Liu, Z., Pan, A., 2006. Conceptual model about the interaction between El Niño/Southern Oscillation and Quasi-Biennial

Oscillation in far west equatorial Pacific. Sci. China Earth Sci. 49 (8), 889.

Losada, I., Reguero, B., Mndez, F., Castanedo, S., Abascal, A., Mnguez, R., 2013. Long-term changes in sea-level components in Latin America and the Caribbean. Glob. Planet. Change 104, 34—50.

Lu, Q., Zuo, J., Li, Y., Chen, M., 2013. Interannual sea level variability in the tropical Pacific Ocean from 1993 to 2006. Glob. Planet. Change 107, 70—81.

Luo, W., Yuan, L., Yu, Z., Yi, L., Xie, Z., 2011. Regional sea level change in Northwestern Pacific: process, characteristic and prediction. J. Geogr. Sci. 21 (3), 387—400.

Masuda, S., Awaji, T., Toyoda, T., Shikama, Y., Ishikawa, Y., 2009. Temporal evolution of the equatorial thermocline associated with the 1991—2006 ENSO. J. Geophys. Res. 114 (C3), C03015.

Nerem, R., 1999. Measuring very low frequency sea level variations using satellite altimeter data. Glob. Planet. Change 20 (23), 157—171.

Nerem, R.S., Leuliette, E., Cazenave, A., 2006. Present-day sea-level change: a review. C. R. Geosci. 338 (14), 1077—1083.

Oliver, E.C.J., Thompson, K.R., 2010. Madden-Julian oscillation and sea level: local and remote forcing. J. Geophys. Res. 115 (C1), C01003.

Ortiz-Tánchez, E., Ebeling, W., Lanius, K., 2002. MEI, SOI and mid-range correlations in the onset of El Niño — Southern Oscillation. Physica A 310 (3/4), 509—520.

Paeth, H., Scholten, A., Friederichs, P., Hense, A., 2008. Uncertainties in climate change prediction: El Niño-Southern Oscillation and monsoons. Glob. Planet. Change 60 (34), 265—288.

Puillat, I., Prevosto, M., Mercier, H., Thomas, S., 2014. Time series analysis of marine data: a key knowledge at the crossroads of marine sciences. J. Mar. Syst. 130, 1—3.

Rong, Z., Liu, Y., Zong, H., Cheng, Y., 2007. Interannual sea level variability in the South China Sea and its response to ENSO. Glob. Planet. Change 55 (4), 257—272.

Singh, P., Chowdary, J., Gnanaseelan, C., 2013. Impact of prolonged La Nia events on the Indian Ocean with a special emphasis on southwest Tropical Indian Ocean SST. Glob. Planet. Change 100, 28—37.

Takahashi, D., Morimoto, A., 2013. Mean field and annual variation of surface flow in the East China Sea as revealed by combining satellite altimeter and drifter data. Prog. Oceanogr. 111, 125—139.

Wang, H., Yang, Z., Saito, Y., Liu, J.P., Sun, X., 2006. Interannual and seasonal variation of the Huanghe (Yellow River) water discharge over the past 50 years: connections to impacts from ENSO events and dams. Glob. Planet. Change 50 (34), 212—225.

Wolter, K., Timlin, M.S., 1998. Measuring the strength of ENSO events: how does 1997/98 rank? Weather 53 (9), 315—324.

Wyrtki, K., 1975. El Niño — the dynamic response of the equatorial Pacific Ocean to atmospheric forcing. J. Phys. Oceanogr. 5 (4), 572—584.

Xu, K., Zhu, C., He, J., 2012. Linkage between the dominant modes in Pacific subsurface ocean temperature and the two type ENSO events. Chin. Sci. Bull. 57 (26), 3491—3496.

Yadav, R., Ramu, D., Dimri, A., 2013. On the relationship between ENSO patterns and winter precipitation over North and Central India. Glob. Planet. Change 107, 50—58.

Yu, Z.Y., Yuan, L.W., Lü, G.N., Luo, W., Xie, Z.R., 2011. Coupling characteristics of zonal and meridional sea level change revealed by satellite altimetry data and their response to ENSO events. Chin. J. Geophys. 54 (8), 1972—1982.

Yuan, L., Yu, Z., Xie, Z., Song, Z., Lü, G., 2009. ENSO signals and their spatial-temporal variation characteristics recorded by the sea-level changes in the Northwest Pacific margin during 1965—2005. Sci. China Earth Sci. 52 (6), 869—882.

Zhang, X., Church, J.A., 2012. Sea level trends, interannual and decadal variability in the Pacific Ocean. Geophys. Res. Lett. 39 (21), L21701.